Bulk Sensitive Soft X-Ray Edge Probing for Elucidation of Charge Compensation in Battery Electrodes

Marcus Fehse,[*,†,‡,¶] Christoph J. Sahle,[§] Matteo P. Hogan,[‖] Chiara Cavallari,[§] Erik M. Kelder,[†,¶] Maria Alfredsson,[‖,¶] and Alessandro Longo[*,‡,⊥]

†*Faculty of Applied Sciences, Delft University of Technology, Delft, Netherlands.*

‡*Dutch-Belgian (DUBBLE), ESRF-The European Synchrotron, Grenoble, France.*

¶*Alistore European Research Institute, CNRS, Amiens, France.*

§*ESRF-The European Synchrotron, Grenoble, France.*

‖*School of Physical Sciences, University of Kent, UK.*

⊥*Istituto per lo Studio dei Materiali Nanostrutturatti (ISMN)-CNR, UOS Palermo, Palermo, Italy*

E-mail: marcus.fehse@umontpellier.fr; alessandro.longo@esrf.fr

Abstract

To this day, elucidating the charge transfer process in electrode material upon electrochemical cycling remains a challenge, primarily due to the complexity of chemical reactions at the electrode surfaces. Here we present an elegant and reliable method to probe bulk sensitive soft edges for elucidating anodic and cathodic charge compensation contribution via x-ray Raman scattering spectroscopy. By using a hard x-ray incident beam this technique circumvents surface limitations and is practically free of self-absorption due to its non-resonant nature. In addition, it does not require complex

sample preparation or experimental setups, making it an ideal tool for potential *in situ* analysis of the electronic structure of electrode materials. In this study we monitored for the first time bulk soft edges of both oxygen and transition metal (iron) of the cathode material Li_2FeSiO_4 during one complete electrochemical cycle concurrently. Our results reveal that the redox mechanism relies primarily on the iron (cathodic) contribution. Nevertheless, a change in electron confinement of the oxygen suggests its active involvement in the charge compensation process (anodic). Moreover, we were able to support the experimentally observed changes of the electronic structure with *ab initio* based simulation.

Keywords

X-ray Raman Scattering; Soft x-ray edges; Li-ion batteries; high voltage cathode materials; anodic charge compensation; Li_2FeSiO_4

1 Introduction

Numerous experimental and theoretical studies have been dedicated to elucidate the complexity of electrochemical redox reactions in battery materials. However, the distinction between surface confined and bulk electrode phenomena remains a subject of controversy and debate. Therefore, there is a strong urge to overcome the limitation of conventional experimental methods and go beyond the theoretical predictions. In this study, we present a reliable and elegant solution to address this challenge.

X-ray absorption spectroscopy (XAS) offers plentiful insights into battery materials and is a standard tool for investigation of diverse electrode materials.[1] Regrettably, absorption K-edges of low Z elements and transition metal (TM) L-edges are cumbersome to access or completely inaccessible with conventional XAS. This is unfortunate as many promising electrode materials comprise these low Z elements (N, O, Si, S, Li, Na, Ca, Al, etc.) and

the majority of cathode electrode materials are based on TM redox centres.[2] X-ray Raman Scattering (XRS) spectroscopy is a unique element specific technique that can circumvent these limitations. It allows direct observation of soft x-ray edges of bulk samples without sophisticated sample preparation thanks to the use of a hard x-ray incident beam ($\approx 10\,\mathrm{keV}$), which is inelastically scattered by the sample.[3] In this way XRS combines the advantages of hard x-ray techniques, i.e. bulk sensitivity, with the sensitivity of soft XAS (sXAS). Unlike XAS, XRS is not limited to dipolar excitations, therefore non-dipole excitations can provide additional information for obtaining full density of projected states. Furthermore, XRS allows the accommodation of complex sample environments and circumvents cumbersome experimental setups under vacuum or inert atmosphere as well as avoids the self-absorption problematic due to the non-resonant nature of this technique, which make sXAS experiments very challenging. The superiority of XRS over the sXAS technique in terms of probing depth and data quality was impressively demonstrated by *Braun et al.* by investigating electronic structure of transition metal cathode material for lithium ion batteries (LIB). In their study the authors highlight that spectroscopic results of bulk XRS and surface confined sXAS greatly differ, underlining the importance of bulk analysis for obtaining an extensive and representative picture of the bulk physicochemical process in electrode materials.[4] Due to its strong photon scattering yield and its prominence, graphite has been the most intensively studied LIB electrode material using XRS.[5–7] Moreover, the capability of XRS to probe Fe L-edge and oxygen K-edge in complex sample environments has been recently demonstrated.[8–10]

Thanks to being composed of abundant, low-cost, environmental benign, and non-toxic elements Li_2FeSiO_4 has received great interest as an alternative cathode material for LIB, since the discovery of its electrochemical activity more than a decade ago.[11] Its stability is at least as high as commercialised $LiFePO_4$ (LFP) but features potentially increased energy and power density owing to the elevated intercalation potential and the faster charge transport.[12–15] Its complex polymorphism has been intensively studied and is mostly under-

stood.[16,17] However, recently the capability of reversibly extracting more than one lithium per formula unit has led to a vivid scientific debate and numerous publications. The initial hypothesis of more than one electron extraction on the basis of Fe(III) to Fe(IV) transformation proposed by *Islam et al.*[18] and experimentally claimed by *Lv et al.*[13] was not supported by later studies.[14,15,19–21] While the formation of Fe(IV) as the origin of additional capacity at elevated voltage has been rebutted, the role of oxygen as active anionic redox agent has shifted into focus of research. Numerous studies have emerged since the first observation of such anionic redox contribution in layered transition metal oxides about five years ago.[22–26] The discovery of an anodic charge contribution was met with enthusiasm by the battery research community, since it holds the promise to boost capacity and energy density of traditional cathode materials. In this regard, an important role of oxygen in the charge compensation at elevated potential has been also proposed for the reversible extraction of more than one lithium from polyanionic Li_2FeSiO_4.[15,19–21,27,28] While *Masese et al.* claim that oxygen charge compensation occurs exclusively during extraction of a second lithium per formula unit,[19] later studies suggest active participation of oxygen already at an earlier stage in the redox process.[27,28] In their recent Density Functional Theory (DFT) calculation based study *Zheng et al.* point out the importance of $3d$ electronic configuration for the involvement of oxygen $2p$ in the charge compensation along with the necessity of oxygen polaron formation.[21]

Unfortunately, all of the previously published studies on the elucidation of charge compensation mechanism in Li_2FeSiO_4 bear inherent drawbacks. On the one hand, the theoretical studies are unable to deliver information on intermediate states of electrochemical process due to intrinsic limitations of functionals. On the other hand, spectroscopic techniques are limited by low penetration depth, unrealistic sample environment, or ambiguity of spectral results. In this regard the surface limitation of soft x-ray absorption spectroscopy is particularly troubling since electrode-electrolyte interfaces are very complex systems, often covered with surface layers (e.g. solid-electrolyte interphase, SEI). Therefore, the outcome of

such surface confined spectroscopic measurements greatly depend on the sample preparation method and conditions.

To overcome the experimental limitations of soft XAS and obtain a more reliable and exhaustive picture of the electronic structure than theoretical studies can provide, we present here a thorough bulk study of anionic O $2p$ and cathodic TM $3d$ electronic states of Li_2FeSiO_4 cathode material at different states during one complete electrochemical cycle using XRS spectroscopy.

2 Experimental

2.1 Sample and Electrode Preparation

Synthesis of electrode material has been described elsewhere.[14] All samples were taken from the same electrode casting batch and have identical electrode loading and composition. The electrode thickness is about 30 μm the particle size is in the sub-micrometer range. The active material electrodes were mounted in electrochemical half-cells with lithium metal as counter and reference electrode. The cells were cycled in EC:DEC (1:1) with 1 M $LiPF_6$ at C/6 rate, whereas 1 C corresponds to deinsertion/ insertion of one lithium per formula unit in one hour, 165 mA g^{-1}. For the *ex-situ* cells used in this experiment the rested and cycled batteries were opened in an argon filled glovebox, electrodes were removed and washed thoroughly with anhydrous ethanol to remove electrolyte remnants and any SEI formed, primarily to minimise the oxygen spectral contribution from carbonate species. The washed electrodes were dried under vacuum and were then vacuum sealed under argon, in laminated pouch cells with aluminium windows (Al thickness 15 μm) in the centre of the pouch on both sides.

2.2 X-ray Raman Scattering

All X-ray Raman scattering (XRS) spectroscopy data were gathered at the beamline ID20 of the ESRF. The pink beam from four U26 undulators was monochromatized using a cryogeni-

cally cooled Si(111) monochromator and focused to a spot size of approximately $10\,\mu m \times 20\,\mu m$ (V × H) at the sample position using a mirror system in Kirkpatrick-Baez geometry. The large solid angle spectrometer at ID20 was used to collect XRS data with 36 spherically bent Si(660) analyser crystals.[29] The data were treated with the XRStools program package as described elsewhere.[30] The *ex situ* electrodes, sealed in pouch cells, were placed at an incident beam angle of $\approx 10\,^\circ$ into the beam. The beam position was verified by the presence of Li 1*s* peak at $\approx 55\,\text{eV}$, see spectra in S.I.. All measurements were collected at room temperature. Acquisition scans lasted around 10-14 h per sample. We collected several scans of the oxygen K-edge by scanning the incident beam energy to create energy losses in the vicinity of the oxygen K-edge. All scans were checked for consistency and signals from different analyser crystals were averaged over. The overall energy resolution was 1.0 eV, and the mean momentum transfer was $6.2 \pm 0.4\,\text{Å}^{-1}$. All spectra have been normalised and a smoothing function has been applied to the spectra presented.

2.3 Simulation

To elucidate the electronic structure of the material, O K-edge *ab initio* simulation were performed using the Finite Difference Method Near Edge Structure (`FDMNES`) software package.[31,32] The simulation have been performed by using the multiple scattering theory based on the muffin-tin approximation on the potential shape on the Green scheme.[33] The muffin-tin radii were tuned to have a good overlap between the different spherical potentials. A non-relativistic calculation was performed and the Hedin-Lundqvist exchange potential was used. The approximation of non-excited absorbing atoms was used which, in this case, best reproduces the experimental data.[34] The semi-empirical parameters `screening` and `dilatorb` were used to reproduce the electronic configuration of the material. In this respect, two matrices of different simulated spectra corresponding to different values of `screening` and `dilatorb` were calculated and a combination of both was matched to the experimental data set for obtaining best agreement. Furthermore, the total density of states (DOS) as well as

the individual projections of p and d-DOS at Oxygen K-edge for the Li_2FeSiO_4 structure[19] were calculated[35] and are reported in S.I..

2.4 X-ray Absorption Spectroscopy

The sample preparation and experimental details for the complementary *operando* Fe K-edge XAS study have been previously reported elsewhere.[14]

3 Results

3.1 X-ray Raman Scattering

A scheme of a typical electrochemical cycling curve of Li_2FeSiO_4 is depicted in Fig. 1, along with seven red markers indicating the state of charge/ discharge of the prepared *post mortem* samples. The charge (delithiation) comprises samples A to E, whereas A corresponds to pristine material, D at the end of charge (EOC) at 4.7 V, and E to EOC held for several hours at 4.8 V to ensure that the oxidation reaction reached equilibrium conditions. The discharge (lithiation) comprises samples D to G, whereas G is the relithiated material after one cycle. Although the discharge was incomplete at this point we will refer to this sample as "end of discharge" (EOD) in the following. Due to experimental issues we were not able to acquire spectra of a sample at a higher degree of discharge.

From the electrochemical cycling curve it is salient that more than the theoretical capacity based on the transition metal redox couple Fe^{2+} / Fe^{3+} is reversibly obtained when cycling beyond 4.2 V vs. Li^+/Li. Typically, not the complete extracted capacity during charge is reversed upon discharge which can be mostly attributed to irreversible lithium extraction and parasitic side reactions of the electrolyte. The latter is particularly strong when cycling at elevated potential, as previously pointed out.[14]

The evolution of the oxygen K-edge upon charge and discharge is shown in Fig. 2. Two main features can be identified. Firstly, the pre-edge peak related to the transition from

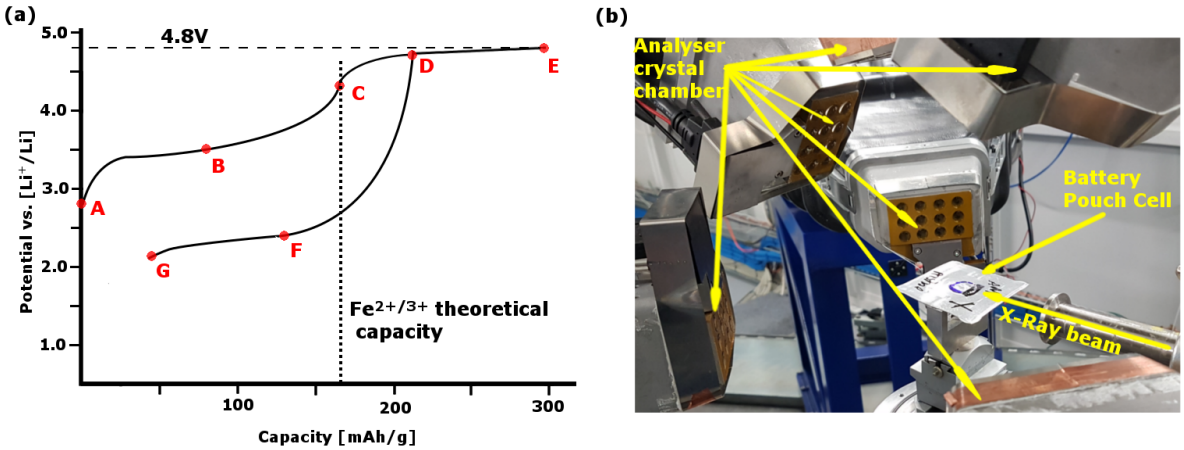

Figure 1: (a) Scheme of electrochemical cycling curve of Li_2FeSiO_4 vs. lithium. Red markers indicate the state of charge /discharge of the seven *post mortem* samples.(b) Experimental setup of pouch cell in grazing XRS.

O $1s$ to the empty Fe $3d$ mixed with O $2p$ orbital at $\approx$ 531 eV. The position is well in line values reported in the literature[36] as well as with our d-DOS projection which illustrate that the pre-edge peak originates primarily from Fe $3d$ states, see S.I.. The evolution of normalised pre-peak area shown in the inset was obtained by single peak fitting of the area marked by the hatched box. Secondly, the broad main peak associated to the excitation of oxygen $1s$ electrons above the Fermi level into the Fe $4sp$ band hybridised with O $2p$ states, centred around $\approx$ 539 eV. The absence of carbonate species in the oxygen spectra confirms the effective removal of SEI by ethanol washing procedure.[37]

Upon charging an increase of the normalised intensity of pre-edge feature is observed which is in good agreement with the recent study by *Lu et al.* applying surface confined soft XAS.[27] According to *Yoon et al.* the pre-edge reveals important information about the hole state distribution and the effective charge on the oxygen atom since the density of empty bound state in molecular energy level is related to the hybridisation of the transition metal $3d$- oxygen $2p$.[38] In this regard the observed increase in intensity, see inset Fig. 2 reflects the emptying of the d-orbitals, resulting from the oxidation of Fe^{+2} to Fe^{+3}. On the contrary to our findings, *Masese et al.* found no change of the pre-edge intensity for the extraction of the first lithium from Li_2FeSiO_4 structure. However, the authors report a strong increase in

the pre-edge intensity for extraction of more than one lithium per formula unit, which is in line with our observation of sample E, held several hours at elevated potential of 4.8 V. The authors attributed this to the formation of O $2p$ ligand holes, reflecting primary contribution of oxygen to the charge compensation process.[19] However, their results are based on *ex situ* fluorescence yield detection XAS with limited number of samples and probing depth which penalises the reliability and representativeness.

Upon discharge the trend of pre-edge intensity increase is partially reversed, as shown in Fig. 2. While the intensity of the pre-edge intensity is effectively reduced upon discharge, at the highest state of discharge (sample G) a more pronounced pre-edge feature than for the pristine sample (A) is maintained. The irreversible phase transition from monoclinic to orthorhombic structure upon first delithiation[17,39] could be partially accountable for the observed discrepancy between the charge and the discharge process.

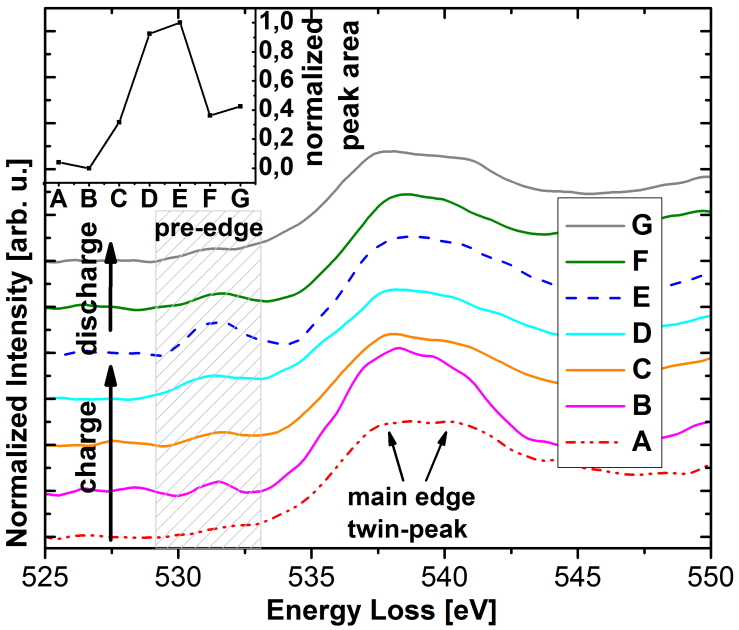

Figure 2: Evolution of oxygen K pre-edge (hatched box) and main edge during charge and discharge of bulk Li_2FeSiO_4 measured via X-ray Raman Scattering. The inset shows the evolution of normalised integrated pre-edge peak area within the hatched box.

To highlight the evolution of O $2p$ main edge spectra, a cumulative and constant stacking

of the spectra acquired during charge (sample A to E) and discharge (sample D to G) are presented in Fig. 3 (a) and (b), respectively. The position of the O $2p$ main edge remains largely unchanged upon electrochemical cycling indicating that oxidation state of lattice oxygen is globally maintained. However, Fig. 3 shows clearly that upon lithium deinsertion a gradual change in intensity ratio of main edge twin peak occurs, which points towards an alteration of oxygen orbitals during Li deinsertion process. Upon lithium reinsertion these changes of the O $2p$ band structure are partially reversed. Nevertheless, the trend is incomplete which could be connected to the fact that the discharge reaction was incomplete at sample G state as well as to the irreversible phase transformation upon first charge.

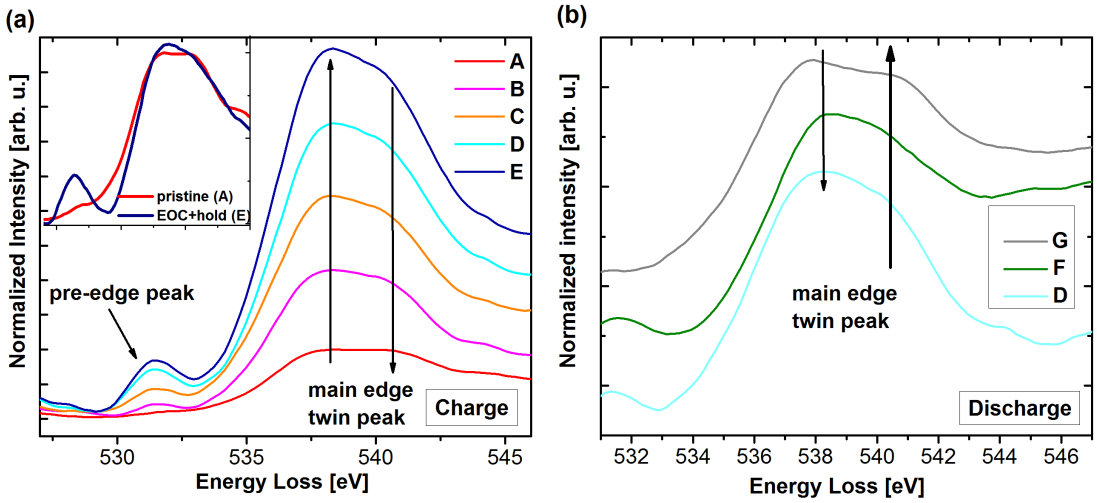

Figure 3: (a) Cumulative stacking of main oxygen K-edge spectra upon charge and inset without stacking. (b) Constant stacking of main oxygen K-edge spectra upon discharge. Arrows indicate the twin-peak intensity ratio changes.

3.2 Soft edge simulation

In order to gain a more fundamental understanding of the electronic structural changes the `FDMNES` code was used to simulate the spectra in an *ab initio* approach. Within this approach, the two semi empirical parameters `dilatorb` and `screening` were systematically adjusted to

reproduce the electronic configuration of the investigated material. The `dilatorb` parameter modifies the valence orbitals by dilating or contracting them, hence allowing one to alter the degree of covalency. This can be very useful for ionic materials to address the ionic species, for instance the oxygen the formal charge of O^{2-} where the atomic bases are calculated for neutral atoms. By changing the `screening` parameter the electronic charge in the non-full valence orbital of the absorber can be modified, by placing an additional electron on the first non-occupied state while the absorbing atom remains (almost) neutral.[40] Two matrices of different simulated spectra corresponding to gradually increasing values of `screening` and `dilatorb` were calculated and are presented in Fig. 4 (a) and (b), respectively. In Fig. 4(a) we show that an increase in `dilatorb` parameter leads primarily to a reduction of the pre-edge feature intensity accompanied by a shift to lower energy. The effect of the `screening` value, pictured in Fig. 4(b), is more complex as it leads to a change in intensity ratio of the pre-edge and main edge feature, but also strongly influences the shape of the latter. In this regard, the change of the intensity ratio of the twin-peak is particularly apparent.

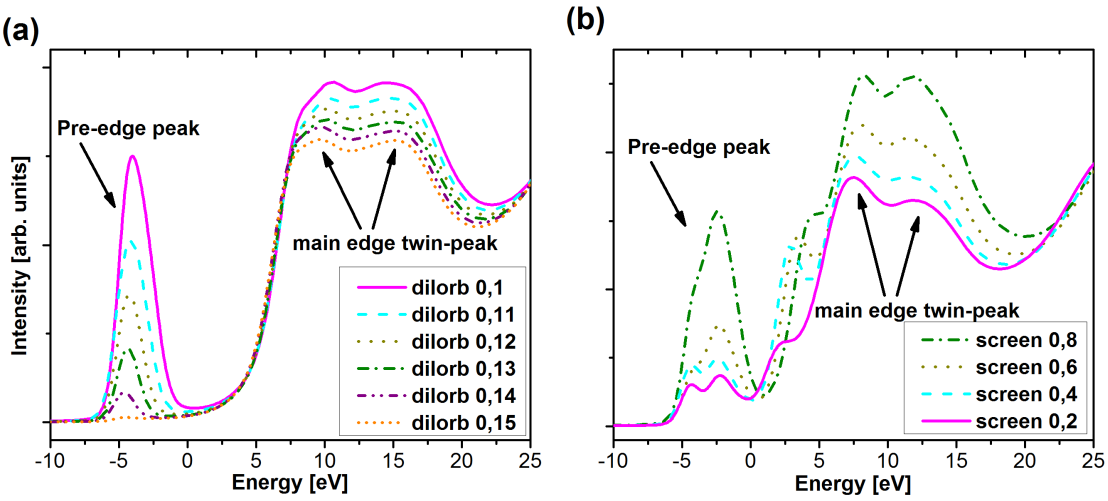

Figure 4: Influence of empirical parameters (a) `dilatorb` which alters covalency and (b) `screening` which changes electron confinement on the simulated spectra of Li_2FeSiO_4 using `FDMNES` code.

Subsequently, for a defined value of `dilatorb` another matrix with different values of

`screening` was simulated in order to achieve best agreement with the three experimental spectra of samples pristine (A), end of charge plus hold (F), and end of discharge (G), see Fig. 5. Within the examined energy range all main features of the electronic band structure around the oxygen K-edge were reasonably well reproduced by applying `dilatorb` value of 0.09, and `screening` values of 0.7, and 0.8 for sample A, and E, respectively. By default the `screening` value is one. The fact that the core hole charge is not completely screened (partial electron charge missing) points to a correlation effect, caused by presence of the excited $3d$ electron, hindering the screening process.[40] The observed change of the `screening` value indicates the modification of the local environment of oxygen upon delithiation. More specifically, the 0.1 increase in `screening` value upon charge reflects a less filled state of the d-orbital, which results in the rise of the pre-edge feature. This reduction in `screening` potential is also accompanied by a reduction in electron confinement of the O $2p$ band resulting in upwards shift of the Fermi level, which is in good agreement with recently published DFT calculations.[21] The observed reduction in electron confinement is furthermore in line with previously reported shortening of Fe–O bond length, arising from an increase in covalency and increased electron delocalisation upon delithiation.[17]

The changes of the shape of the O $2p$ main edge during charge and discharge, which are shown in Fig. 3, reflect the rearrangement of oxygen orbitals and the redistribution of charge during electrochemical lithium extraction and insertion. The fact that the intensity ratio of the twin-peak can be partially reproduced using the `screening` parameter, shown in Fig. 4(b), connotes that the observed changes are linked to a change in electron confinement and a $3d$ electron correlation effect upon charge. A lowering of electron confinement at the oxygen upon charge implies an increased sharing of the charge with the transition metal. In this sense the observed changes in electronic structure suggests that oxygen provides charge for the Fe^{2+} / Fe^{3+} redox couple throughout the electrochemical reaction which could sustain the reversible extraction of more than one lithium per formula unit. Regrettably, the resolution of the experimental data not allow us to interpret the O $2p$ spectra in more detail.

For the sample at lowest state of discharge (sample G), best agreement of simulation and experimental data was achieved applying the same value of `screening` as for the pristine sample (A). This implies that changes of electron confinement are largely reversible. Nevertheless, a slightly elevated `dilatorb` value was found, indicating a change in covalency of the bond.

The disagreement of the simulated spectra compared to experimental data for the energy range beyond the main edge features stems from the complex data extraction process. In the here presented results the emphasis of data extraction procedure lay on elucidating the energy range of pre-edge feature. By adequately adjusting the extraction parameters a better agreement for the spectra beyond first O $2p$ feature can be achieved. However, this comes as a trade-off for the agreement in the pre-edge feature range. In this regard, it should be also noted that the electrode samples in pouch cell assembly used for this spectroscopic investigation were optimised for their electrochemical performance and not for scattering yield.

3.3 Fe L-edge

Similarly to the O K-edge, XRS was used to probe the Fe L_3-edges. L-edges are arguably the most direct probe of TM redox activity. Besides formal valence the $3d$ L-edges fingerprint the spin-state as well as chemical bond configuration via the $2p$ to $3d$ electron excitation. The evolution of Fe L_3-edge spectra upon charge and discharge of Li_2FeSiO_4 are illustrated in Fig. 6 (a) and (b), respectively. The spectra of the Fe L_3-edge which derives from the $2p_{3/2} \rightarrow 3d$ transition is composed of two main features centred at 708.2 and 709.8 eV. Upon charge a change of peak intensity ratio from $\approx$ 708 to 710 eV is observed. This is in good agreement with evolution of pre-edge features of Fe K-edge upon charge shown in the inset of Fig. 6a. Please refer to the S.I. for complete XANES spectra and enlarged version pre-edge evolution graph. The good agreement between complementary iron K-edge XAS results and L-edge XRS underline that XRS is an effective and reliable method to probe electron transition

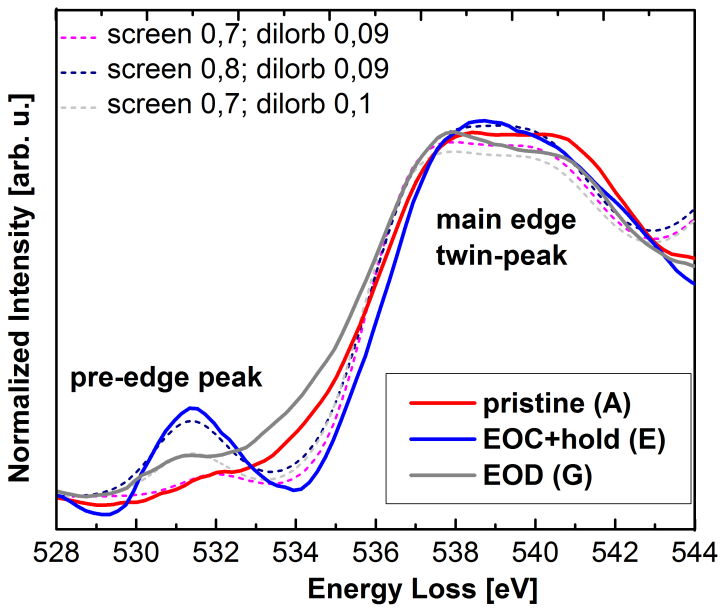

Figure 5: Experimental spectra (solid lines) and FDMNES simulated spectra (dotted lines) of the oxygen K-edge of Li_2FeSiO_4 of pristine (sample A), end of charge + holding at 4.8 V (EOC+hold, sample E) and end of discharge (EOD, sample G).

of redox active *d*-orbitals via direct $2p \rightarrow 3d$ transition of the L-edge, with the benefit of significantly higher intensity than indirect dipole forbidden $1s \rightarrow 3d$ K-edge pre-edge features via XAS. The observed peak intensity shift is well in line with the values reported in the literature for a $Fe^{2+} \rightarrow Fe^{3+}$ transformation.[2,27,41,42] The continuous increase of Fe^{3+} peak for the sample held at elevated potential (E) indicates that the oxidation from the ferrous to the ferric state was incomplete at sample D stage, which can be attributed to kinetic hindrance due to sluggish charge transfer.[43] Although the experimental resolution does not allow us to exclude the oxidation beyond Fe(III) with certainty, the formation of Fe(IV) has been rebutted by a complementary *operando* XANES analysis, see S.I., as well as in multiple other studies.[15,19–21] It should be noted that the pristine sample contained a slight share of Fe^{3+} originating from phase impurities.

Upon discharge the changes of the Fe L_3-edge are only partially reversed and the initial state of pristine is not recovered, analogously to our observation for the O K-edge, see Fig.

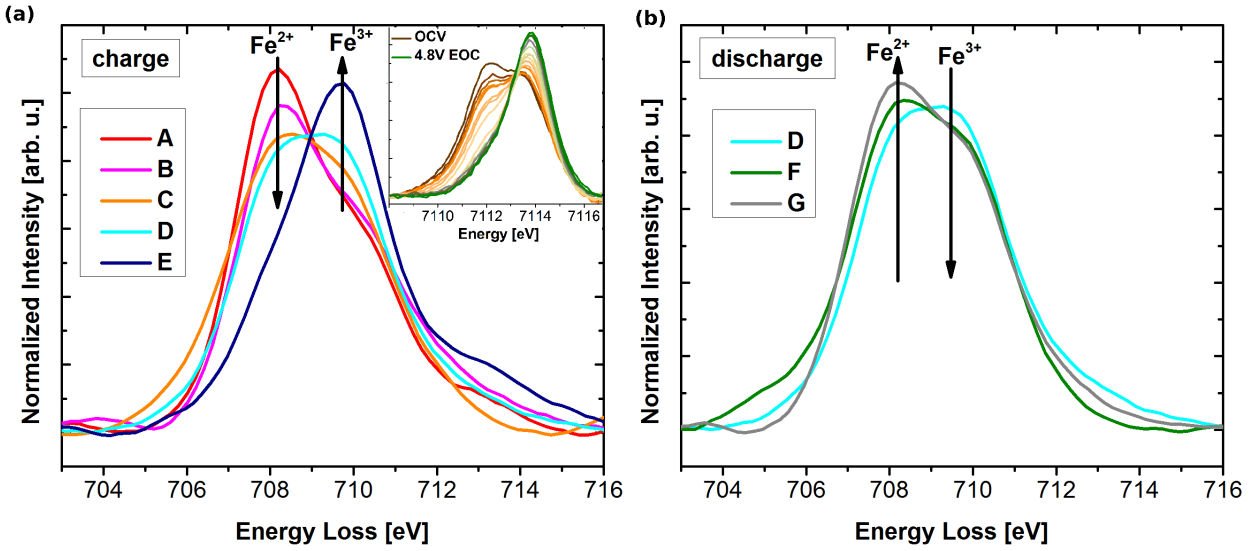

Figure 6: Iron L_3-edge evolution during (a) charge and (b) discharge of Li_2FeSiO_4 measured via X-ray Raman Scattering. The inset depicts evolution of Fe K-edge pre-edge features obtained via XAS, see S.I. for enlarged version.

6(b), inset of Fig. 2, and Fig. 3(b), respectively. This irreversibility is attributed to the incomplete state of discharge of sample G, as well as irreversible structural transformation during initial charge, *vide supra*.Fig. 6(b), inset of Fig 2, and Fig. 3(b), respectively

4 Discussion

The above presented results highlight the effectiveness and usefulness of X-ray Raman scattering spectroscopy for accessing bulk electronic structure information to elucidate the complex electrochemical charge transfer process in electrode materials. Additionally we demonstrate that the observed electronic structural changes can be reproduced for intermediate states of charge by the `FDMNES` code which could have been hardly achieved applying DFT calculations. In detail, our results show that the electrochemical activity of Li_2FeSiO_4 is primarily based on $Fe^{2+/3+}$ redox centre. XRS reveals a reversible shift in Fe L_3 edge corresponding to the oxidation of Fe^{2+} to Fe^{3+}, which are supported by complementary XAS results. Furthermore, XRS allowed us to monitor the change in occupancy of the hybridised oxygen orbitals which result in a change of intensity of the oxygen K-edge pre-edge fea-

ture. Moreover, our findings show that the charge distribution of oxygen changes during the lithium extraction process, notably an increased delocalisation of oxygen electron at EOD. Whether the alteration of the main edge is also linked the enhanced metal-oxygen hybridisation or indicates an additional charge compensation by lending electrons to the $Fe^{2+/3+}$ redox couple, can not be answered with certainty based on these results. Although the role of oxygen can not be determined beyond doubt within this study, it is certain that it plays an important role for preserving electronic and structural stability of the host material by preventing the formation of unstable Fe^{4+}. The oxygen contribution suggested by our XRS spectroscopy analysis is therefore much more subtle and uncertain than previously claimed in calculation-based predictions[15,21,28] or surface confined soft XAS[19,27] studies which somewhat frivolously attribute changes of oxygen pre-edge feature directly to anodic charge contribution instead of metal-oxygen hybridisation. We like to highlight that our findings represent bulk electrode information and reflect therefore the electronic structure of lattice elements of the full electrode. Nevertheless, a major anodic charge compensation that would explain most of the additional reversible capacity observed was not confirmed by our study. Therefore, previously suggested phenomena such as rich surface chemistry are to be considered to explain the observed additional capacity.[14,44]

By using a pouch cell assembly we demonstrated that the XRS technique offers the possibility to work under sample relevant conditions with the potential of carrying out experiments *in situ* configuration. Nevertheless, the challenge of overlapping spectral contribution from other oxygen containing battery components (electrolyte, SEI, etc.) needs to be addressed. Also, the reduction of background scattering and increase of signal-to-noise ratio is a crucial requirement for reduced acquisition time that would permit *operando* measurements. The recently published *in situ* XRS study on Li intercalation in graphite using a confocal-like setup is an encouraging step in this direction.[45]

Improving energy resolution of XRS spectroscopy remains a challenge for complex samples such as electrode materials due to strong parasitic scattering. Tailored sample holders

which effectively shield non-desired scattering contribution could lead to much increased signal-to-noise ratio which will enhance reliability as well as reduce acquisition time.

Interestingly, XRS also allows the combination of depth profiling as well as 2D mapping which could be coupled to perform a 3D screening of an electrode, unveiling exciting insights on propagation of electrochemical reaction front propagation.[46,47]

5 Conclusion

We have demonstrated that X-ray Raman scattering spectroscopy can be conveniently applied to probe bulk soft x-ray edges of both anionic and cathodic redox pairs to elucidate the charge transfer process upon electrochemical cycling in battery materials. For the first time we applied XRS to closely follow the change in electronic structure of polyanionic cathode material Li_2FeSiO_4, monitoring the evolution of O $2p$ and Fe $3d$ orbitals concurrently at distinct points during one complete electrochemical cycle, without cumbersome sample preparation or the need for sophisticated sample environment. Furthermore, we show that the `FDMNES` code is a suitable tool to reproduce soft edge spectra of intermediate states of the redox reaction, allowing deeper insights into the electronic structural changes. Our findings reveal a gradual emptying and filling of $3d$ orbitals upon charge and discharge, respectively, reflecting the primary redox activity of the transition metal. Besides the evident enhanced metal-oxygen hybridisation reflected by the oxygen pre-edge rise, the changes of charge distribution of O $2p$ could not be attributed with certainty. To the best of our knowledge the XRS spectroscopy presented in this study is currently the only available technique that allows studying soft edge electronic structures of bulk materials. Thus, providing the scientific battery community with a tool to elucidate the ambiguity between surface vs. bulk as well as unveiling anionic charge compensation contribution of low Z elements on the bulk level of electrode materials.

Acknowledgements

Alistore-European Research Institute is gratefully acknowledged for financial support through the postdoc grant to M. Fehse. ESRF and NWO are acknowledged for providing synchrotron radiation beamtime at beamline ID20 and BM26A, respectively. The authors furthermore like to thank Y. Joly for valuable comments and suggestion concerning the `FDMNES` simulation.

Supporting Information

XRS spectra of quasi-elastic scattering and inelastic Li 1*s* peaks. Projection of individual and total density of states for O K-edge of Li_2FeSiO_4. *Operando* Fe K-edge XANES during first charge of Li_2FeSiO_4.

References

References

(1) Fehse, M.; Iadecola, A.; Sougrati, M. T.; Conti, P.; Giorgetti, M.; Stievano, L. Applying chemometrics to study battery materials: Towards the comprehensive analysis of complex operando datasets. *Energy Storage Mater.* **2019**, *18*, 328–337.

(2) Li, Q.; Qiao, R.; Wray, L. A.; Chen, J.; Zhuo, Z.; Chen, Y.; Yan, S.; Pan, F.; Hussain, Z.; Yang, W. Quantitative probe of the transition metal redox in battery electrodes through soft x-ray absorption spectroscopy. *J. Phys. D. Appl. Phys.* **2016**, *49*, 413003.

(3) Sternemann, C.; Wilke, M. Spectroscopy of low and intermediate Z elements at extreme conditions: in situ studies of Earth materials at pressure and temperature via X-ray Raman scattering. *High Press. Res.* **2016**, *7959*, 1–18.

(4) Braun, A.; Nordlund, D.; Song, S.-W. W.; Huang, T.-W. W.; Sokaras, D.; Liu, X.; Yang, W.; Weng, T.-C. C.; Liu, Z. Hard X-rays in-soft X-rays out: An operando piggyback view deep into a charging lithium ion battery with X-ray Raman spectroscopy. *J. Electron Spectros. Relat. Phenomena* **2015**, *200*, 257–263.

(5) Schülke, W.; Berthold, A.; Kaprolat, A.; GÌĹntherodt, H. J. Evidence for interlayer band shifts upon lithium intercalation in graphite from inelastic x-ray scattering. *Phys. Rev. Lett.* **1988**, *60*, 2217–2220.

(6) Balasubramanian, M.; Johnson, C. S.; Cross, J. O.; Seidler, G. T.; Fister, T. T.; Stern, E. A.; Hamner, C.; Mariager, S. O. Fine structure and chemical shifts in nonresonant inelastic x-ray scattering from Li-intercalated graphite. *Appl. Phys. Lett.* **2007**, *91*, 031904.

(7) Stutz, G. E.; Otero, M.; Ceppi, S. A.; Robledo, C. B.; Luque, G.; Leiva, E.; Barraco Díaz, D. E. Intercalation stage dependence of core electronic excitations in Li-intercalated graphite from inelastic X-ray scattering. *Appl. Phys. Lett.* **2017**, *110*, 253901.

(8) Nyrow, A.; Sternemann, C.; Tse, J. S.; Weis, C.; Sahle, C. J.; Mende, K.; Wieland, D. C.; Cerantola, V.; Gordon, R. A.; Spiekermann, G.; Regier, T.; Wilke, M.; Tolan, M. Bulk sensitive determination of the Fe3+/Fe Tot-ratio in minerals by Fe L2/3-edge X-ray Raman scattering. *J. Anal. At. Spectrom.* **2016**, *31*, 815–820.

(9) Longo, A.; Liotta, L. F.; Banerjee, D.; La Parola, V.; Puleo, F.; Cavallari, C.; Sahle, C. J.; Moretti Sala, M.; Martorana, A. The Effect of Ni Doping on the Performance and Electronic Structure of LSCF Cathodes Used for IT-SOFCs. *J. Phys. Chem. C* **2018**, *122*, 1003–1013.

(10) Firet, N. J.; Venugopal, A.; Blommaert, M. A.; Cavallari, C.; Sahle, C. J.; Longo, A.; Smith, W. A. Chemisorption of anionic species from the electrolyte alters the surface

electronic structure and composition of photocharged BiVO4. *Chem. Mater.* **2019**, acs.chemmater.9b02121.

(11) Nytén, A.; Abouimrane, A.; Armand, M.; Gustafsson, T.; Thomas, J. O. Electrochemical performance of Li2FeSiO4 as a new Li-battery cathode material. *Electrochem. commun.* **2005**, *7*, 156–160.

(12) Zhou, F.; Cococcioni, M.; Kang, K.; Ceder, G. The Li intercalation potential of LiMPO4 and LiMSiO4 olivines with M = Fe, Mn, Co, Ni. *Electrochem. commun.* **2004**, *6*, 1144–1148.

(13) Lv, D.; Bai, J.; Zhang, P.; Wu, S.; Li, Y.; Wen, W.; Jiang, Z.; Mi, J. J.; Zhu, Z.; Yang, Y. Understanding the high capacity of Li2FeSiO4: In situ XRD/XANES study combined with First principles calculations. *Chem. Mater.* **2013**, *25*, 2014–2020.

(14) Brownrigg, A. W.; Mountjoy, G.; Chadwick, A. V.; Alfredsson, M.; Bras, W.; Billaud, J.; Armstrong, a. R.; Bruce, P. G.; Dominko, R.; Kelder, E. M. In situ Fe K-edge X-ray absorption spectroscopy study during cycling of Li 2 FeSiO 4 and Li 2.2 Fe 0.9 SiO 4 Li ion battery materials. *J. Mater. Chem. A* **2015**, *3*, 7314–7322.

(15) Sarkar, T.; Bharadwaj, M. D.; Waghmare, U. V.; Kumar, P. Mechanism of Charge Transfer in Olivine-Type LiFeSiO4 and LiFe0.5M0.5SiO4 (M = Mg or Al) Cathode Materials: First-Principles Analysis. *J. Phys. Chem. C* **2015**, *119*, 9125–9133.

(16) Dominko, R. Li2MSiO4 (M = Fe and/or Mn) cathode materials. *J. Power Sources* **2008**, *184*, 462–468.

(17) Eames, C.; Armstrong, A. R.; Bruce, P. G.; Islam, M. S. Insights into changes in voltage and structure of Li 2FeSiO 4 polymorphs for lithium-ion batteries. *Chem. Mater.* **2012**, *24*, 2155–2161.

(18) Islam, M. S.; Dominko, R.; Masquelier, C.; Sirisopanaporn, C.; Armstrong, A. R.; Bruce, P. G. Silicate cathodes for lithium batteries: alternatives to phosphates? *J. Mater. Chem.* **2011**, *21*, 9811–9818.

(19) Masese, T.; Tassel, C.; Orikasa, Y.; Koyama, Y.; Arai, H.; Hayashi, N.; Kim, J.; Mori, T.; Yamamoto, K.; Kobayashi, Y.; Kageyama, H.; Ogumi, Z.; Uchimoto, Y. Crystal structural changes and charge compensation mechanism during two lithium extraction/insertion between Li2FeSiO4 and FeSiO4. *J. Phys. Chem. C* **2015**, *119*, 10206–10211.

(20) Liivat, A.; Thomas, J.; Guo, J.; Yang, Y. Novel insights into higher capacity from the Li-ion battery cathode material Li2FeSiO4. *Electrochim. Acta* **2017**, *223*, 109–114.

(21) Zheng, J.; Teng, G.; Yang, J.; Xu, M.; Yao, Q.; Zhuo, Z.; Yang, W.; Liu, Q.; Pan, F. Mechanism of Exact Transition between Cationic and Anionic Redox Activities in Cathode Material Li2FeSiO4. *J. Phys. Chem. Lett.* **2018**, *9*, 6262–6268.

(22) Sathiya, M.; Rousse, G.; Ramesha, K.; Laisa, C. P.; Vezin, H.; Sougrati, M. T.; Doublet, M. L.; Foix, D.; Gonbeau, D.; Walker, W.; Prakash, A. S.; Ben Hassine, M.; Dupont, L.; Tarascon, J. M. Reversible anionic redox chemistry in high-capacity layered-oxide electrodes. *Nat. Mater.* **2013**, *12*, 827–835.

(23) Koga, H.; Croguennec, L.; Menetrier, M.; Douhil, K.; Belin, S.; Bourgeois, L.; Suard, E.; Weill, F.; Delmas, C. Reversible Oxygen Participation to the Redox Processes Revealed for Li1.20Mn0.54Co0.13Ni0.13O2. *J. Electrochem. Soc.* **2013**, *160*, A786–A792.

(24) McCalla, E.; Sougrati, M. T.; Rousse, G.; Berg, E. J.; Abakumov, A.; Recham, N.; Ramesha, K.; Sathiya, M.; Dominko, R.; Van Tendeloo, G.; Novák, P.; Tarascon, J. M. Understanding the Roles of Anionic Redox and Oxygen Release during Electrochemical Cycling of Lithium-Rich Layered Li4FeSbO6. *J. Am. Chem. Soc.* **2015**, *137*, 4804–4814.

(25) McCalla, E. et al. Reversible Li-Intercalation through Oxygen Reactivity in Li-Rich Li-Fe-Te Oxide Materials. *J. Electrochem. Soc.* **2015**, *162*, A1341–A1351.

(26) Saubanère, M.; McCalla, E.; Tarascon, J. M.; Doublet, M. L. The intriguing question of anionic redox in high-energy density cathodes for Li-ion batteries. *Energy Environ. Sci.* **2016**, *9*, 984–991.

(27) Lu, X.; Chiu, H. C.; Arthur, Z.; Zhou, J.; Wang, J.; Chen, N.; Jiang, D. T.; Zaghib, K.; Demopoulos, G. P. Li-ion storage dynamics in metastable nanostructured Li2FeSiO4cathode: Antisite-induced phase transition and lattice oxygen participation. *J. Power Sources* **2016**, *329*, 355–363.

(28) Zhang, P.; Wei, S. H. Origin of charge compensation and its effect on the stability of oxide cathodes for Li-ion batteries: The case of orthosilicates. *Electrochim. Acta* **2018**, *270*, 409–416.

(29) Huotari, S.; Sahle, C. J.; Henriquet, C.; Al-Zein, A.; Martel, K.; Simonelli, L.; Verbeni, R.; Gonzalez, H.; Lagier, M. C.; Ponchut, C.; Moretti Sala, M.; Krisch, M.; Monaco, G. A large-solid-angle X-ray Raman scattering spectrometer at ID20 of the European Synchrotron Radiation Facility. *J. Synchrotron Radiat.* **2017**, *24*, 521–530.

(30) Sahle, C. J.; Mirone, A.; Niskanen, J.; Inkinen, J.; Krisch, M.; Huotari, S. Planning, performing and analyzing X-ray Raman scattering experiments. *J. Synchrotron Radiat.* **2015**, *22*, 400–409.

(31) Joly, Y. X-ray absorption near-edge structure calculations beyond the muffin-tin approximation. *Phys. Rev. B - Condens. Matter Mater. Phys.* **2001**, *63*, 125120.

(32) Joly, Y.; Cavallari, C.; Guda, S. A.; Sahle, C. J. Full-Potential Simulation of X-ray Raman Scattering Spectroscopy. *J. Chem. Theory Comput.* **2017**, *13*, 2172–2177.

(33) Guda, S. A.; Guda, A. A.; Soldatov, M. A.; Lomachenko, K. A.; Bugaev, A. L.; Lamberti, C.; Gawelda, W.; Bressler, C.; Smolentsev, G.; Soldatov, A. V.; Joly, Y. Optimized Finite Difference Method for the Full-Potential XANES Simulations: Application to Molecular Adsorption Geometries in MOFs and Metal-Ligand Intersystem Crossing Transients. *J. Chem. Theory Comput.* **2015**, *11*, 4512–4521.

(34) Ankudinov, A. L.; Rehr, J. J.; Low, J. J.; Bare, S. R. Sensitivity of Pt x-ray absorption near edge structure to the morphology of small Pt clusters. *J. Chem. Phys.* **2002**, *116*, 1911–1919.

(35) Rehr, J. J.; Kas, J. J.; Vila, F. D.; Prange, M. P.; Jorissen, K. Parameter-free calculations of X-ray spectra with FEFF9. *Phys. Chem. Chem. Phys.* **2010**, *12*, 5503–5513.

(36) Orikasa, Y.; Masese, T.; Koyama, Y.; Mori, T.; Hattori, M.; Yamamoto, K.; Okado, T.; Huang, Z.-D.; Minato, T.; Tassel, C.; Kim, J.; Kobayashi, Y.; Abe, T.; Kageyama, H.; Uchimoto, Y. High energy density rechargeable magnesium battery using earth-abundant and non-toxic elements. *Sci. Rep.* **2015**, *4*, 5622.

(37) Fister, T. T.; Schmidt, M.; Fenter, P.; Johnson, C. S.; Slater, M. D.; Chan, M. K.; Shirley, E. L. Electronic structure of lithium battery interphase compounds: Comparison between inelastic x-ray scattering measurements and theory. *J. Chem. Phys.* **2011**, *135*, 224513.

(38) Yoon, W.-S.; Balasubramanian, M.; Chung, K. Y.; Yang, X.-Q.; McBreen, J.; Grey, C. P.; Fischer, D. A. Investigation of the Charge Compensation Mechanism on the Electrochemically Li-Ion Deintercalated Li ₁ ₋ _x Co _{1/3} Ni _{1/3} Mn _{1/3} O ₂ Electrode System by Combination of So. *J. Am. Chem. Soc.* **2005**, *127*, 17479–17487.

(39) Armstrong, A. R.; Kuganathan, N.; Islam, M. S.; Bruce, P. G. Structure and lithium

transport pathways in Li2FeSiO4cathodes for lithium batteries. *J. Am. Chem. Soc.* **2011**, *133*, 13031–13035.

(40) Joly, Y.; Cabaret, D.; Renevier, H.; Natoli, C. Electron Population Analysis by Full-Potential X-Ray Absorption Simulations. *Phys. Rev. Lett.* **1999**, *82*, 2398–2401.

(41) Van Aken, P. A.; Liebscher, B.; Styrsa, V. J. Quantitative determination of iron oxidation states in minerals using Fe L2,3-edge electron energy-loss near-edge structure spectroscopy. *Phys. Chem. Miner.* **1998**, *25*, 323–327.

(42) Nagasaka, M.; Yuzawa, H.; Horigome, T.; Hitchcock, A. P.; Kosugi, N. Electrochemical reaction of aqueous iron sulfate solutions studied by Fe L-edge soft X-ray absorption spectroscopy. *J. Phys. Chem. C* **2013**, *117*, 16343–16348.

(43) Qu, L.; Luo, D.; Fang, S.; Liu, Y.; Yang, L.; Hirano, S. I.; Yang, C. C. Mg-doped Li2FeSiO4/C as high-performance cathode material for lithium-ion battery. *J. Power Sources* **2016**, *307*, 69–76.

(44) Dominko, R.; Sirisopanaporn, C.; Masquelier, C.; Hanzel, D.; Arcon, I.; Gaberscek, M. On the Origin of the Electrochemical Capacity of Li2Fe0.8Mn0.2SiO4. *J. Electrochem. Soc.* **2010**, *157*, A1309.

(45) Nonaka, T.; Kawaura, H.; Makimura, Y.; Nishimura, Y. F.; Dohmae, K. In situ X-ray Raman scattering spectroscopy of a graphite electrode for lithium-ion batteries. *J. Power Sources* **2019**, *419*, 203–207.

(46) Huotari, S.; Pylkkänen, T.; Verbeni, R.; Monaco, G.; Hämäläinen, K. Direct tomography with chemical-bond contrast. *Nat. Mater.* **2011**, *10*, 489–493.

(47) Sahle, C. J.; Mirone, A.; Vincent, T.; Kallonen, A.; Huotari, S. Improving the spatial and statistical accuracy in X-ray Raman scattering based direct tomography. *J. Synchrotron Radiat.* **2017**, *24*, 476–481.